JOURNAL OF THEORETICAL AND APPLIED MECHANICS
52, 1, pp. 189-197, Warsaw 2014

FORCED VIBRATIONS ANALYSIS OF A CONICAL SLEEVE-SHAFT FRICTION JOINT

Andrzej Andrzejuk, Zbigniew Skup, Robert Zalewski
Warsaw University of Technology, Institute of Machine Design Fundamentals, Warszawa, Poland
e-mail: mang@ipbm.simr.pw.pl; zskup@ipbm.simr.pw.pl; robertzalewski@wp.pl

The paper presents a theoretical study of the damping process of non-linear vibrations in a one-mass model of a mechanical system over a friction joint. The problem is considered assuming a uniform unit pressure distribution between the contacting surfaces of the conical sleeve-shaft neck of the friction joint. The steady-state motion of the system is subject to harmonic excitation. The analysis includes the following: the influence of geometric parameters of the system, its external load amplitude, unit pressures and the friction coefficient upon the amplitude-frequency characteristics and the phase-frequency characteristics. Structural friction has been also taken into account. The equation of motion of the examined mechanical system has been solved by means of the slowly varying parameters (Van der Pol) method and a numerical simulation method.

Key words: conical joint, sleeve-shaft neck, energy dissipation, structural friction

1. Introduction

Forced vibration problems of mechanical systems with structural friction are widely discussed in a number of domestic and foreign scientific papers, see Andrzejuk (2012), Gałkowski (1999), Giergiel (1990), Grudziński and Kostek (2005), Kosior (2005), Mostowicz-Szulewski and Nizioł (1992), Osiński (1998), Skup (2010), Zboiński and Ostachowicz (2001) or Badraghan (1994), Meng (1989), Sanitruk *et al.* (1997), Sextro (2002), Wang and Chen (1993), Zahavi (1993).

Analytical considerations presented in this paper concern a real model of a friction joint (Fig. 1). It consists of two cooperating conical friction pairs (Fig. 2). Such types of joints have found an extensive application in different types of mechanical systems and devices. They are often designed and manufactured as natural energy dissipation elements.

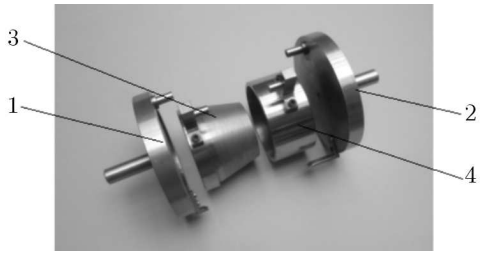

Fig. 1. Components of the investigated sleeve-shaft neck friction joint: 1 – lower pressure plate grip of the model, 2 – upper grip of the model, 3 – shaft neck, 4 – sleeve

Mathematical description of structural friction phenomena is not easy due to the complexity of the friction process and difficulties in describing the state of stresses and deformations occurring in cooperating elements. Therefore, the description is based on simplified assumptions and fundamental mechanical laws that apply to the patterns of stress and deformations resulting from tension, compression, torsion, shearing. A typical approach to such problems can be found

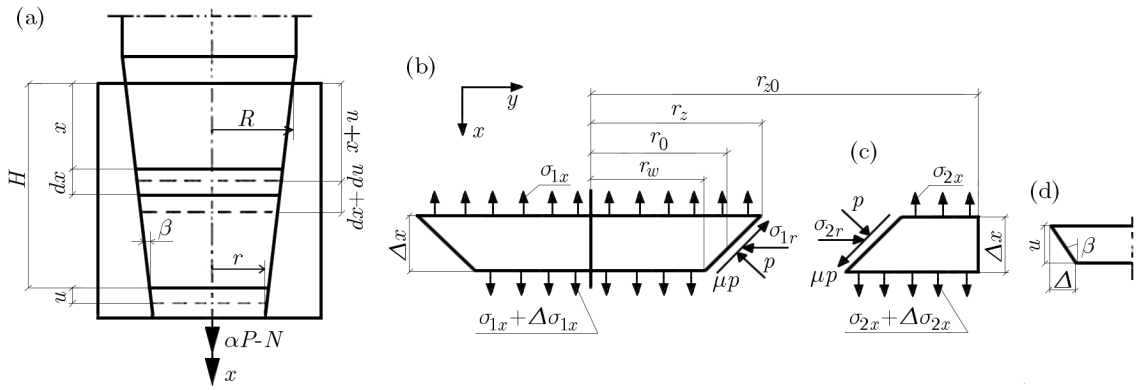

Fig. 2. Physical model: (a) sleeve-shaft neck joint; (b) element of thickness Δx at a distance x from the larger end of the shaft; (c) element of thickness Δx at a distance x from the larger end of the sleeve; (d) displacement

in Gałkowski (1999), Kosior (2005), Osiński (1998), Skup (2010). The following assumptions were made in order to analyze the investigated model: the distribution of unit pressure between cooperating surfaces of the joint contact elements is uniform; there is a constant friction coefficient of the contacting elements for an arbitrary value of the unit pressure; friction force on contact surfaces of the cooperating elements is subject to Coulomb's law; and, consequently, the frictional resistance is proportional to the pressure, while the material properties are described by Hook's law. The friction is fully developed in the sliding zone, the internal forces are neutral (due to very low acceleration values) and, finally, the cross-sectional area of the cooperating elements remains flat. Besides theoretical investigations of the model shown in Fig. 2, also experimental tests on the real testing object (Fig. 1) have been carried out.

2. A mathematical model of the friction joint – analysis of forced vibration

In this Section, the solution of the problem concerning forced vibrations of the conical friction joint is presented. Nonlinear vibrations of the examined elements under forced harmonic loading (2.1) are examined. An additional assumption has been made that the considered friction joint can be described as a single-mass system with a triangular hysteresis loop

$$P = P_0 \cos \omega t \tag{2.1}$$

The mathematical analysis is carried out considering the Van der Pol method.

The equation of motion of the system can be written as follows

$$m\ddot{u} + P(u, \operatorname{sgn} \dot{u}) = P_0 \cos \omega t \tag{2.2}$$

where m is the reduced mass, u – axial displacement; $P(u, \operatorname{sgn} \dot{u})$ – force represented by the structural hysteretic loop (Fig. 3) dependent on the relative displacement, amplitude and sign of velocity, P_0 – excitation amplitude of the loading force, t – time; ω – angular velocity of the excitation force.

Assuming the approximation of (2.2) in the form

$$u = A \cos(\omega t + \phi) \tag{2.3}$$

where ϕ denotes the initial forcing phase A, ϕ – slowly varying time functions.

Differentiating equation (2.3), we obtain

$$\dot{u} = \dot{A} \cos(\omega t + \phi) - A\omega \sin(\omega t + \phi) - A\dot{\phi} \sin(\omega t + \phi) \tag{2.4}$$

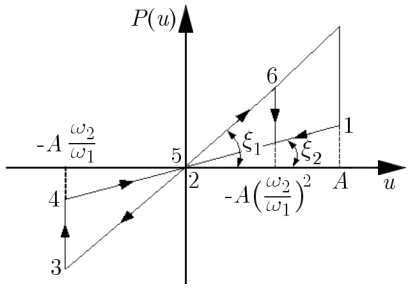

Fig. 3. Hysteresis loop for the investigated friction joint

By analogy to the Lagrange method of parameters variation, (2.4) may be written in the form

$$\dot{A}\cos(\omega t+\phi)-A\dot{\phi}\sin(\omega t+\phi)=0 \tag{2.5}$$

Therefore

$$\dot{u}=-A\omega\sin(\omega t+\phi) \tag{2.6}$$

Thus differentiating (2.6) once again, gives

$$\ddot{u}=-\dot{A}\omega\sin(\omega t+\phi)-A\omega^2\cos(\omega t+\phi)-A\omega\dot{\phi}\cos(\omega t+\phi) \tag{2.7}$$

After introducing the denotation

$$z=\omega t+\phi \tag{2.8}$$

and taking advantage of (2.7), differential equation (2.2) takes the form

$$-\dot{A}\omega\sin z-A\omega^2\cos z-A\omega\dot{\phi}\cos z+\frac{P(u,\,\mathrm{sgn}\,\dot{u})}{m}=\frac{P_0}{m}\cos(z-\phi) \tag{2.9}$$

Multiplying equation (2.5) by $-\omega\cos z$ and equation (2.9) by $\sin z$, we obtain

$$\begin{aligned}&\dot{A}\omega\cos^2 z-A\omega\dot{\phi}\sin z\cos z=0\\&\dot{A}\omega\sin^2 z+A\omega^2\sin z\cos z+A\omega\dot{\phi}\sin z\cos z-\frac{P(u,\,\mathrm{sgn}\,\dot{u})}{m}\sin z=-\frac{P_0}{m}\sin z\cos(z-\phi)\end{aligned} \tag{2.10}$$

Subtracting the system of equations (2.10), gives

$$\dot{A}\omega+A\omega^2\sin z\cos z-\frac{P(u,\,\mathrm{sgn}\,\dot{u})}{m}\sin z=-\frac{P_0}{m}\sin z\cos(z-\phi) \tag{2.11}$$

Since A and ϕ_0 are slowly varying parameters in equation (2.2), equation (2.11) takes, after integrating over the interval $z\in(0,2\pi)$, the following form

$$\dot{A}\omega\int_0^{2\pi}dz+A\omega^2\int_0^{2\pi}\sin z\cos z\,dz-\frac{1}{m}\int_0^{2\pi}P(u,\,\mathrm{sgn}\,\dot{u})\sin z\,dz=-\frac{P_0}{m}\int_0^{2\pi}\sin z\cos(z-\phi)\,dz \tag{2.12}$$

Integrating both sides of equation (2.12), we get

$$2\pi\dot{A}\omega-\frac{1}{m}\int_0^{2\pi}P(u,\,\mathrm{sgn}\,\dot{u})\sin z\,dz=-\frac{P_0\pi}{m}\sin\phi \tag{2.13}$$

Multiplying equation (2.5) by $\omega \sin z$ and equation (2.9) by $\cos z$, one arrives at the following system of equations

$$\begin{aligned} &\dot{A}\omega \sin z \cos z - A\omega\dot{\phi}\sin^2 z = 0 \\ &-\dot{A}\omega \sin z \cos z - A\omega^2 \cos^2 z - A\omega\dot{\phi}\cos^2 z + \frac{P(u,\, \mathrm{sgn}\,\dot{u})}{m}\cos z = \frac{P_0}{m}\cos z \cos(z-\phi) \end{aligned} \tag{2.14}$$

Adding both sides of equations (2.14) and averaging over one cycle of $z \in (0, 2\pi)$, gives

$$-2\pi A\omega\dot{\phi} - \pi A\omega^2 + \frac{1}{m}\int_0^{2\pi} P(u,\, \mathrm{sgn}\,\dot{u})\cos z\; dz = \frac{P_0\pi}{m}\cos\phi \tag{2.15}$$

Steady-state equations (2.13) and (2.15) can be obtained when $\dot{A} = \dot{\phi} = 0$, therefore these equations are reduced to the form

$$\begin{aligned} &\sin\phi = \frac{1}{P_0\pi}\int_0^{2\pi} P(u,\, \mathrm{sgn}\,\dot{u})\sin z\; dz \\ &m\omega^2 + \frac{P_0}{A}\cos\phi = \frac{1}{\pi A}\int_0^{2\pi} P(u,\, \mathrm{sgn}\,\dot{u})\cos z\; dz \end{aligned} \tag{2.16}$$

Integrating equations (2.16) produces a discontinuity of $P(u, \mathrm{sgn}\,\dot{u})$ for $\dot{\phi} = 0$. To avoid this problem, we confine our considerations to a single half-period (the motion between four stops).

Thus, the integration interval (from 0 to 2π) of the right-hand terms of the above equations is divided into four sub-intervals. A similar procedure has been successfully adopted in Badraghan (1994), Gałkowski (1999), Giergiel (1990), Kosior (2005), Osiński (1998) or Skup (2010). The influence of elasto-frictional parameters k_1 and k_2, corresponding to $\tan\xi_1$ and $\tan\xi_2$, on the investigated system is depicted in Fig. 3

$$k_1 = \tan\xi_1 = \frac{P_1}{u_{max}} \qquad k_2 = \tan\xi_2 = \frac{P_2}{u_{max}} \qquad u_{max} = A \tag{2.17}$$

where

$$P_1 = \alpha_1 P \qquad P_2 = \alpha_2 P \qquad \alpha_1 = 1 \tag{2.18}$$

Basing on the work by Skup (2010), the maximal axial displacement u_{max} and dimensionless parameter α_2 are given by

$$u_1(x = H) = u_{max} = \alpha_1 P(m_{17} + m_{18}) \qquad \alpha_2 = \alpha_1\frac{m_{17} + m_{18}}{m_{19} + m_{18}} \tag{2.19}$$

where

$$\begin{aligned} &m_{17} = \frac{\eta_3 \tan\beta(\lambda_9 R^{\lambda_{10}-\lambda_9} r^{\lambda_9} - \lambda_{10} r^{\lambda_{10}})}{\pi r(r^{\lambda_{10}} - R^{\lambda_{10}-\lambda_9} r^{\lambda_9})} \qquad m_{18} = \frac{\eta_4}{\pi r} \\ &m_{19} = \frac{\eta_9 \tan\beta(\lambda_{11} R^{\lambda_{12}-\lambda_{11}} r^{\lambda_{11}} - \lambda_{12} r^{\lambda_{12}})}{\pi r(r^{\lambda_{12}} - R^{\lambda_{12}-\lambda_{11}} r^{\lambda_{11}})} \end{aligned}$$

and

$$\eta_1 = \frac{\chi}{E_2}\Big[1-\nu_2+\frac{r_{z0}^2}{r^2}(1+\nu_2)\Big]+\frac{1-\nu_1}{E_1} \qquad \eta_2 = \frac{\cos\beta(1-\mu\tan\beta)}{2(\tan\beta+\mu)\tan\beta}$$

$$\eta_3 = \eta_1\eta_2 \qquad \eta_4 = \frac{\nu_1}{E_1}\tan\beta$$

$$\chi = \frac{1}{\Big(\frac{r_{z0}}{r}\Big)^2-1} \qquad \eta_8 = \frac{\cos\beta(1+\mu\tan\beta)}{2\tan\beta(\tan\beta-\mu)}$$

$$\eta_9 = \eta_1\eta_8 \qquad \Delta_{41} = B_4^2+4C_{12}>0$$

$$\lambda_{9,10} = \frac{B_4\mp\sqrt{\Delta_{41}}}{2} \qquad B_4 = 1+\frac{\eta_6}{\eta_3\tan\beta}$$

$$C_{12} = \frac{\eta_7}{\eta_3\tan^2\beta} \qquad \eta_6 = \eta_4-2\eta_3\tan\beta-\eta_5$$

$$\eta_7 = \eta_4\tan\beta+\frac{1}{E_1} \qquad \eta_5 = \frac{\nu_1\cos\beta(1-\mu\tan\beta)}{E_1(\tan\beta+\mu)}$$

$$\Delta_{43} = B_5^2+4C_{15}>0 \qquad \lambda_{11,12} = \frac{B_5\mp\sqrt{\Delta_{43}}}{2}$$

$$B_5 = 1+\frac{\eta_{10}}{\eta_9\tan\beta} \qquad C_{15} = \frac{\eta_{11}}{\eta_9\tan^2\beta}$$

$$\eta_{10} = \eta_4-2\eta_9\tan\beta-c_1 \qquad \eta_{11} = \eta_4\tan\beta+\frac{1}{E_1}$$

$$c_1 = \frac{\nu_1\cos\beta(1+\mu\tan\beta)}{E_1(\tan\beta-\mu)}$$

I Stage of motion from 0 to $\pi/2$, $P(u,\operatorname{sgn}\dot{u})=k_2u$, $\dot{u}<0$, $u>0$.
II Stage of motion from $\pi/2$ to π, $P(u,\operatorname{sgn}\dot{u})=k_1u$, $\dot{u}<0$, $u<0$.
III Stage of motion from π to $3\pi/2$, $P(u,\operatorname{sgn}\dot{u})=k_2u$, $\dot{u}>0$, $u<0$.
IV Stage of motion from $3\pi/2$ to 2π, $P(u,\operatorname{sgn}\dot{u})=k_1u$, $\dot{u}>0$, $u>0$.

Therefore, substituting formulas (2.3), (2.8) and (2.18) into equations (2.16) and integrating, gives

$$\begin{aligned}
&\int_0^{2\pi} P(u,\operatorname{sgn}\dot{u})\sin z\,dz = \int_0^{\frac{\pi}{2}} k_1u\sin z\,dz+\int_{\frac{\pi}{2}}^{\pi} k_2u\sin z\,dz+\int_{\pi}^{\frac{3\pi}{2}} k_1u\sin z\,dz\\
&\quad+\int_{\frac{3\pi}{2}}^{2\pi} k_2u\sin z\,dz = A(k_2-k_1)\\
&\int_0^{2\pi} P(u,\operatorname{sgn}\dot{u})\cos z\,dz = \int_0^{\frac{\pi}{2}} k_1u\cos z\,dz+\int_{\frac{\pi}{2}}^{\pi} k_2u\cos z\,dz+\int_{\pi}^{\frac{3\pi}{2}} k_1u\cos z\,dz\\
&\quad+\int_{\frac{3\pi}{2}}^{2\pi} k_2u\cos z\,dz = \frac{\pi A(k_2+k_1)}{2}
\end{aligned} \tag{2.20}$$

Finally, form (2.20), the expression for (2.16) is given by

$$\sin\phi = \frac{1}{P_0\pi}A(k_2-k_1) \qquad m\omega^2+\frac{P_0}{A}\cos\phi = \frac{k_1+k_2}{2} \tag{2.21}$$

To introduce a dimensionless vibration amplitude to the system of equations (2.21), the following notation was assumed: A – vibration amplitude, a – dimensionless vibration amplitude,

x_{st} – static axial displacement in form of the relative displacement of the friction joint elements, k_i – elasticity of the frictional parameters $(i = 1, 2)$, Δk – dimensionless damping parameter, ω_0 – frequency of free vibrations of the system, γ – dimensionless frequency, k_{av} – average elasticity of the system, k – dimensionless elasticity parameter of the frictional joint. Additionally

$$k_{av} = \frac{k_1 + k_2}{2} \qquad \Delta k = \frac{k_1 - k_2}{k_r} = \frac{2(1-k)}{1+k} \qquad k = \frac{k_2}{k_1} = \frac{P_2}{P_1}$$

$$\omega_0 = \sqrt{\frac{k_{av}}{m}} \qquad \gamma = \frac{\omega}{\omega_0} \qquad k_{st} = \frac{P_0}{k_{av}}$$

$$a = \frac{A}{k_{st}} \qquad \frac{\omega_2}{\omega_1} = \sqrt{\frac{k_2}{k_1}} = \sqrt{k}$$

Therefore

$$\sin\phi = -\frac{a\Delta k}{\pi} \qquad \gamma^2 + \frac{1}{a}\cos\phi = 1 \tag{2.22}$$

With the help of the above equations (2.22), the relation between the tangent of the phase displacement angle ϕ and the dimensionless amplitude a can be calculated as

$$\tan\phi = -\frac{\Delta k}{\pi(1-\gamma^2)} \qquad a = \frac{1}{\sqrt{(1-\gamma^2)^2 + \left(\frac{\Delta k}{\pi}\right)^2}} \tag{2.23}$$

3. Numerical results

Numerical results for vibrations of the considered system have been obtained using the Mathematica environment. Typical results are depicted in Figs. 4-7. The basic geometrical parameters and material properties of the investigated frictional model are presented in Table 1.

Table 1. Parameters of the investigated model

No.	Parameter [unit]	Value
1	Loading force $P_1 = P$ [kN]	100
2	Dimensionless parameter α_1	1
3	Dimensionless parameter α_2 for $\beta = 12°$	0.200
4	Dimensionless parameter α_2 for $\beta = 14°$	0.272
5	Dimensionless parameter α_2 for $\beta = 16°$	0.298
6	Dimensionless parameter α_2 for $\beta = 18°$	0.341
7	Poisson's ratio ν	0.29
8	Young's modulus E [N/mm^2]	$2.1 \cdot 10^5$
9	Friction coefficient μ	0.15
10	Coning angle of tilt β [°]	12, 14, 16, 18
11	External radius of sleeve r_z [mm]	42
12	Internal radius of shaft r_w [mm]	28.03
14	Surface of cross-section field model [mm^2]	2063.3
15	Reduced mass m [kg]	2.661

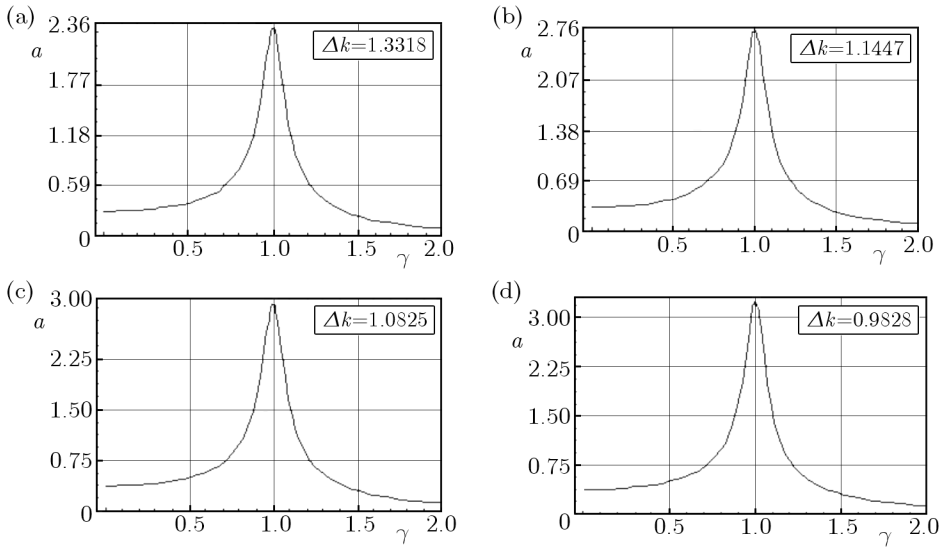

Fig. 4. Typical amplitude-frequency characteristics for forced vibrations of the investigated system and various angles β: (a) 12°, (b) 14°, (c) 16°, (d) 18°

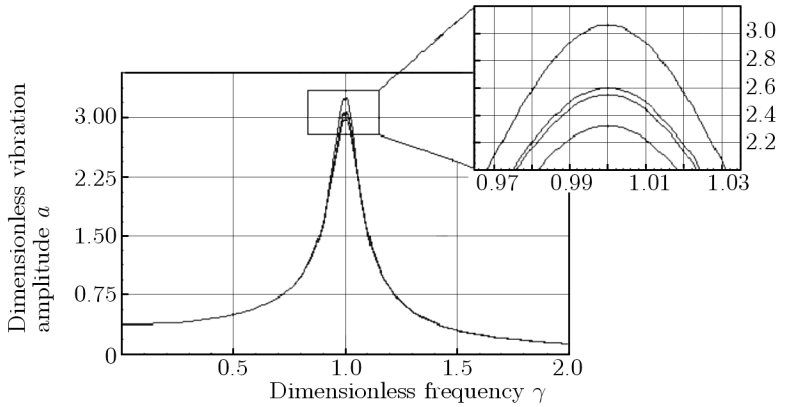

Fig. 5. Global dimensionless amplitude-frequency characteristics for forced vibrations of the investigated system and various values of angle β: 1 – 12°, 2 – 14°, 3 – 16°, 4 – 18°

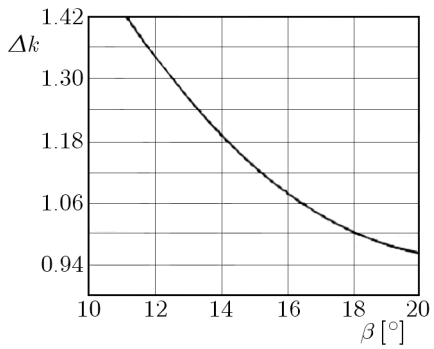

Fig. 6. Relationship between the dimensionless damping parameter Δk and the angle β [°]

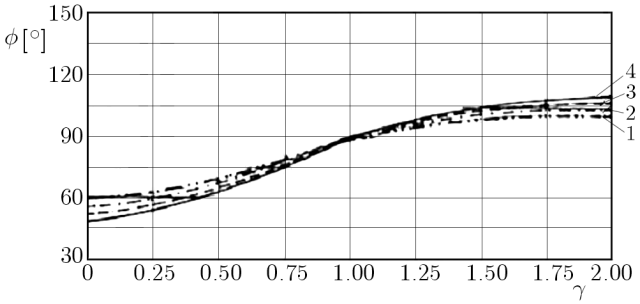

Fig. 7. Graphs of the phase displacement angle ϕ of forced vibration of the friction joint as function of the dimensionless frequency γ for various values of the angle β and dimensionless elasticity k; 1 – $\beta = 12°$, $k = 0.028$, 2 – $\beta = 14°$, $k = 0.099$, 3 – $\beta = 16°$, $k = 0.159$, 4 – $\beta = 18°$, $k = 0.209$

The numerical results for basic parameters of forced vibrations are presented in Table 2.

Table 2. Numerical data

Angle β [°]	Force P_1 [N]	Force P_2 [N]	Displacement u_{max} [mm]	Dimensionless damping parameter Δk	Dimensionless elasticity k
12	100000	20053.2	0.1055	1.3318	0.2005
14	100000	27182.1	0. 0900	1.1447	0.2718
16	100000	29766.6	0.0851	1.0825	0.2977
18	100000	34101.2	0.0755	0.9828	0.3410

4. Concluding remarks

Basing on detailed analysis of the acquired numerical data it was found that all resonance characteristics of dimensionless amplitudes start at 0.33-0.42 range (accordingly to Δk parameter) and tend asymptotically to zero in the post resonance range. In this range, the characteristics exhibit a strong dynamical decrease in the amplitude values. Moreover, the increase in the resonance amplitudes and the rightwards shift of the resonance can be observed for higher cone angles (Figs. 4 and 5) while the other parameters remain unchanged.

Nonlinearities of investigated systems are observable for all considered amplitudes and vibration frequencies. For the forced frequency ω, which is close to the natural frequency of vibrations, non-dimensional amplitudes a assume higher values. Basing on the data depicted in Figs. 4 and 5), the most dangerous range of frequencies for the investigated frictional joint is $0.85 < \gamma < 1.15$.

Values of the dimensionless damping parameter Δk and dimensionless rigidity k (Table 2) strongly depend on the angle β. These characteristics reveal a nonlinear character (Fig. 6). The parameter Δk can be treated as a measure of damping of vibrations of the mechanical system. For higher values of the parameter Δk, the system reveal higher dissipative properties (higher values of the resonance amplitude damping). This phenomenon is observable in Figs. 4 and 5. For lower values of the angle β and parameter k, a decrease in the resonance amplitude values is observed (Fig. 5). Such a phenomenon results from the increasing surface of the micro-sliding zone of the cooperating elastic elements. The selection of the angle β should also take into account the undesirable jamming phenomenon (where $\tan\beta > \mu$).

Relationships of the phase shift ϕ and dimensionless frequency γ for various angles β are depicted in Fig. 7. For higher angles β (lover sliding zone of the cooperating elements) the angle ϕ nearby $\gamma = 1$ rapidly changes. For lower γ, ϕ angle remains small, thus vibrations

are almost in phase with the excitation. For higher γ, an increase in ϕ is observable, tending to 180° regardless of the damping intensity. The phase displacement angle reflects the magnitude of damping in the system. Higher values of the angle ϕ results in an increase in the damping properties of the system.

The best effect of damping of vibrations is observable for a selected value of the friction force. Then the micro-sliding zone of the cooperating parts of the conical joint is greater. Concluding, the damping of vibrations in the investigated system depends on the following parameters: forced amplitude, the rigidity of the shaft and sleeve in the joint, unit pressure and friction coefficient.

References

1. Andrzejuk A., 2012, Analytical and experimental research of a conical sleeve-shaft friction joint (in Polish), *Kwartalnik PTSK*, **3**, 1
2. Badraghan F., 1994, Slip damping in vibrating layered beams and leaf springs; energy dissipated and optimum considerations, *Journal of Sound and Vibration*, **174**, 91-103
3. Gałkowski Z., 1999, Influence of structural friction of the vibrations sleeve-shaft (in Polish), *Science of Books Rzeszów University of Technology*, **174**, 283-288
4. Giergiel J., 1990, *Damping of Mechanical Vibrations* (in Polish), Polish Publishers of Science, Warsaw
5. Grudziński K., Kostek R., 2005, Influence of normal micro-vibrations in contact on sliding motion of solid body, *Journal of Theoretical and Applied Mechanics*, **43**, 37-49
6. Kosior A., 2005, *Influence of Parameters of Joints with Structural Friction on Elastic and Damping Properties of Mechanical Systems* (in Polish), Publishing House of the Warsaw University of Technology, Mechanics, Exercise book, 209
7. Meng C., H., 1989, Modeling and vibration analysis of friction joints, *Journal of Vibration, Acoustics, Stress and Reliability in Design*, **111**, 71-76
8. Mostowicz-Szulewski J., Nizioł, J., 1992, Forced steady-state and non-stationary vibrations of a beam with bilinear hysteretic and hysteretic in fixing, *Nonlinear Vibration Problems*, **24**, 33-62
9. Osiński Z., 1998, *Damping of Vibrations*, A.A. Balkema/Rotterdam/Brookfield
10. Sanitruk K.Y., Imregun M., Ewins D.J., 1997, Harmonic balance vibration analysis of turbine blades with friction dampers, *Journal of Vibration and Acoustics*, **119**, 96-103
11. Sextro W., 2002, *Dynamical Contact Problems with Friction*, Springer, Berlin
12. Skup Z., 2010, *Nonlinear Phenomena in the Damping Vibration* (in Polish), Publishing House of the Warsaw University of Technology, pp. 376
13. Wang J.H., Chen W.K., 1993, Investigation of the vibration of a blade with friction damper by HBM, *Journal of Gas Turbines and Power*, **115**,. 294-299
14. Zahavi E., 1993, Contact problems with friction in machine design, *Computers and Structures*, **48**, 4, 591-594
15. Zboiński G., Ostachowicz W., 2001, Three-dimensional elastic and elasto-plastic frictional contact analysis of turbo-machinery blade attachments, *Journal of Theoretical and Applied Mechanics*, **39**, 3, 769-790

Manuscript received June 26, 2013; accepted for print September 2, 2013